Acta Cryst. (1997). A**53**, 63–73

The Origin of Resonance Scattering in RHEED: Beyond the Tight-Binding Model

S. L. DUDAREV* AND M. J. WHELAN

Department of Materials, University of Oxford, Parks Road, Oxford OX1 3PH, England. E-mail: sergei.dudarev@materials.oxford.ac.uk

(Received 24 May 1996; accepted 13 September 1996)

Abstract

The results are presented of analytical and numerical study of elastic reflection high-energy electron diffraction (RHEED) from a crystalline surface, which show that the positions of the resonance parabolas in RHEED patterns are related to the positions of the peaks of the one-dimensional effective density of states associated with the motion of the incident electron in the direction normal to the surface. This illustrates a fundamental difference between resonance scattering of electrons and Bragg diffraction, the origin of the latter being known to be associated with the existence of forbidden gaps in the spectrum of the density of states. It is also shown that there are cases where the number of resonance parabolas observed in a RHEED pattern exceeds the number of surface states that can be identified for a given surface.

1. Introduction

Recent experimental developments in reflection high-energy electron diffraction (RHEED) and reflection electron microscopy, as well as widespread application of these techniques to the study of structure and dynamic processes on crystal surfaces, have generated considerable interest in problems associated with the theoretical interpretation of electron diffraction patterns observed at grazing incidence (Larsen & Dobson, 1987). Since 1933 (Kikuchi & Nakagawa, 1933), it has been known that the appearance of the brightest features seen in RHEED patterns is associated with the so-called resonance scattering of electrons from surfaces, *i.e.* with a process the origin of which has recently been discussed in a number of publications by Ichimiya, Kambe & Lehmpfuhl (1980), Cowley (1982), Marten & Meyer-Ehmsen (1985), Meyer-Ehmsen (1987) and Lehmpfuhl & Dowell (1986) [for a review of earlier work see Dudarev & Whelan (1996)]. Peng & Cowley (1986), Wang (1989) and Ma & Marks (1989) considered theoretical aspects of the problem of resonance scattering using multislice and Bloch-wave formalisms. Spence & Kim (1987) considered possible application of resonance scattering to adatom-site determination. Bleloch, Howie, Milne & Walls (1989) analysed the dependence of energy-loss spectra on the angle of incidence in the vicinity of resonance conditions. James, Bird & Wright (1989) and James (1990) considered the link between resonance effects observed in transmission and reflection geometries of diffraction. Gajdardziska-Josifovska & Cowley (1991) have considered the geometry of resonance parabolas while Smith, Lehmpfuhl & Uchida (1992) carried out computer simulations of resonance effects in convergent-beam RHEED patterns. Zuo & Liu (1992) studied convergent-beam RHEED patterns and simulated the results using a truncated potential model. Zhao & Tong (1993) carried out extensive numerical analysis of the solution of RHEED equations corresponding to resonance orientations. Experimental investigations of resonance scattering have demonstrated that it leads to the appearance of bright parabolas in RHEED patterns similar to those shown in Fig. 1, and recently it has been found by Reginski, Lamin, Mashanov, Pchelyakov & Sokolov (1995) that diffraction conditions corresponding to resonance reflection of electrons from a surface are particularly suitable for observation of RHEED intensity oscillations during expitaxial growth.

In the past, several alternative explanations have been put forward for the origin of resonance parabolas. Marten & Meyer-Ehmsen (1985) suggested that resonance effects could be explained in terms of monolayer resonances assuming that electrons are diffracted into bound states of a single-atom layer parallel to the surface and that they are channelled inside a layer before being diffracted back into the vacuum region [a generalization of this model to the case of bilayer resonances has been recently considered by Horio & Ichimiya (1996)]. This model seemed to explain well the results obtained for the (111) surface of platinum (Marten & Meyer-Ehmsen, 1985). However, it remained somewhat inconsistent, since one- or two-dimensional states bound by the potential of a single plane or a row of atoms do not represent the true eigenstates of the Schrödinger equation describing motion of the incident electron in the potential of the crystal. In particular, the approximation adopted by Marten & Meyer-Ehmsen (1985) makes it impossible to say whether the bound states

ISSN 0108-7673

involved in the formulation of the model should be considered as surface or bulk states.

Later, Peng & Cowley (1986) attributed the appearance of resonance parabolas to resonance scattering of electrons *via* surface states (Peng & Cowley, 1986), *i.e.* they assumed that the origin of RHEED resonances is associated with the same process of scattering as that which is known in low-energy electron diffraction [see *e.g.* reviews by McRae (1979) and by Echenique & Pendry (1989)]. However, recent demonstration by Dudarev & Whelan (1993, 1994*a*,*b*,*c*, 1995) of the fact that the intensity of some of the resonance peaks can be calculated quantitatively using a tight-binding approach in which tunnelling between states confined by neighbouring potential wells was neglected [which essentially represents a generalization of Meyer-Ehmsen's (1987) model to the case of a sequence of atomic planes containing tightly bound states] has shown that at least in some cases the presence of surface states is not essential.

The latter statement has been questioned by Peng (1994) who noted that the tight-binding approximation is not applicable to some cases (indeed, it follows from examination of the geometry of resonance parabolas that some of them result from scattering involving states, the energy of which lies above the maximum of the potential of the crystal), and who argued, on the basis of the results of numerical simulation, that the appearance of resonance peaks is associated with degeneracy of bulk Bloch states, a condition that was thought to be equivalent to the existence of a surface state (Peng, 1994).

The question that therefore remains to be answered is that, if tunnelling through potential wells separating tightly bound states is included in the formulation of the model (leading therefore to the transformation of the tightly bound states into actual eigenstates of the relevant Schrödinger equation), what effect will this have on the shape and the position of resonance parabolas in RHEED patterns? For example, this point concerns 'intermediate' resonating states corresponding to negative total energy that at the same time exceeds the maximum of the potential of the crystal. Obviously, these states cannot be treated using the tight-binding picture but they are included in the consideration given below.

In this paper, we attempt to answer the above question and to analyse the problem of the origin of the resonance parabolas using an integral-equations approach proposed by Kambe (1967) and examine the arguments that have been proposed recently by various authors (Dudarev & Whelan, 1993, 1995; Peng, 1994). The details of the mathematical formalism involved are described in a recent review by Dudarev & Whelan (1996). The use of integral equations has the advantage of being semi-analytical, *i.e.* within the framework of this approach one can identify the parameters responsible for the appearance of resonance peaks of surface reflectivity without solving the equations themselves. Our analytical results have been obtained using the two-rod approximation proposed by Ohtsuki (1968). Since here we are concerned with obtaining a qualitative answer to the question formulated above, we confine our analysis to the case of relatively large grazing angles of incidence where resonance effects associated with a particular **g** vector can be separated from other effects. In the case of small grazing angles of incidence, we have not been able to identify a parameter using which an analytical treatment might be developed. This leaves numerical methods as the only option available for studying RHEED at relatively low grazing angles of incidence.

In the case of large grazing angles of incidence, we compare the result of analytical study with the result of numerical computations carried out using a many-rod approach, the reliability of which has been recently confirmed by comparison with the methods developed by other researchers (Ichimiya, 1995).* Our main

* A comparison of rocking curves calculated using various numerical methods has been recently carried out by A. Ichimiya, who found that the 'rocking curves calculated [independently] by Dudarev, Korte, Maksym and Peng are nearly exactly the same'.

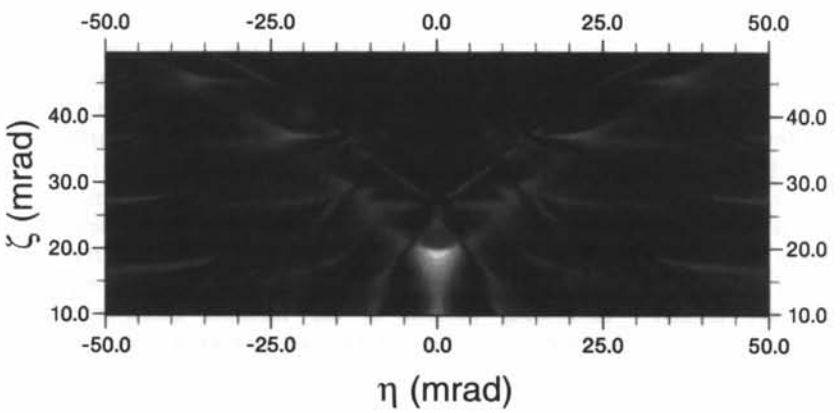

Fig. 1. A 'convergent-beam'-like RHEED pattern calculated for the Pt (111) surface for the direction of incidence close to the $\langle 11\bar{2} \rangle$ axis using five rods [the zero-order (000) rod and the first two side rods on either side of it, $\pm(2\bar{2}0)$, $\pm(4\bar{4}0)$] belonging to the two-dimensional zero-order Laue zone for $E = 100$ keV. The distribution of intensity shown in this figure gives the dependence of intensity of the specular beam as a function of two angles of incidence. Note two double parabolas emerging from the centre of the pattern and ending near upper right and left corners of the picture, respectively.

conclusion is that the arguments employed in the study of the tight-binding model (Dudarev & Whelan, 1994*a*) can be extended to a more general case by making use of some analytical properties of the Green function of the one-dimensional Schrödinger equation. We find that the appearance of resonance parabolas in RHEED patterns is associated with the peaks of the effective one-dimensional density of states corresponding to the motion of an electron in the direction normal to the surface. These peaks correspond to the bands of bulk Bloch states as well as to surface states provided that the latter can be identified for a given surface. Our conclusion becomes trivial in the limiting case where tunnelling between states localized in neighbouring potential wells can be neglected (in which case, no distinction can be made between bulk and surface states), and at the same time it provides new information in the case where the effect of tunnelling is substantial. We show that the 'surface-state' hypothesis cannot explain the origin of all the resonance parabolas that are observed in RHEED diffraction patterns.

2. The kinematics of resonance scattering

We start from a qualitative consideration that illustrates the more rigorous treatment described below. Despite its relative simplicity, this purely kinematical consideration makes it possible to introduce almost all the parameters that determine the position and intensity of the resonance parabolas in a RHEED pattern. Let a high-energy electron be incident from $z \to -\infty$ on a crystal surface, which is assumed to be parallel to the plane $z = 0$. Denote the projection of the wave vector $\mathbf{k}$ of the incident electron on the (x, y) plane by $\mathbf{k}_\parallel$, so that $\mathbf{k} = (\mathbf{k}_\parallel, k_z)$. The wave vector of the electrons specularly reflected from the surface is given by $\mathbf{k} = (\mathbf{k}_\parallel, -k_z)$. If we neglect the periodicity of the potential of the crystal in the (x, y) plane parallel to the surface, the process of scattering can be represented in the form of superposition of free motion parallel to the surface (the energy $E_\parallel^{(0)}$ associated with which is equal to $\hbar^2\mathbf{k}_\parallel^2/2m$) and one-dimensional motion in the laterally averaged potential $U_0(z)$. The energy of this one-dimensional motion towards and away from the surface is given by $E_z^{(0)} = \hbar^2 k_z^2/2m$ and, for any glancing incidence angle ζ, $k_z = k\sin\zeta$, so that the quantity $E_z^{(0)}$ is always positive.

Now consider the effects associated with the periodicity of the crystal potential in the x and y directions. The optical potential $U(\mathbf{r}) = U'(\mathbf{r}) + iU''(\mathbf{r})$ (the imaginary part of which results from inelastic scattering and the influence of surface disorder (Dudarev, Peng & Whelan, 1992, 1995) can be expanded as a two-dimensional Fourier series

$$U(\mathbf{r}) = \sum_{\mathbf{g}'} U_{\mathbf{g}'}(z)\exp(i\mathbf{g}'\cdot\mathbf{R}), \qquad (1)$$

where $\mathbf{R} = (x, y)$ is a two-dimensional vector parallel to the surface of the crystal and $\mathbf{g}'$ is a reciprocal-lattice vector of the two-dimensional lattice. The two-dimensional periodicity of the potential gives rise to elastic scattering involving discrete momentum transfers $\hbar\mathbf{g}'$ parallel to the plane of the surface. Consider the process of scattering associated with a particular reciprocal-lattice vector $\mathbf{g}$ parallel to the surface. As a result of diffraction, the electron is accelerated (or decelerated) in the direction parallel to the surface, so that the (x, y) projection of its wave vector after the scattering is given by $\mathbf{k}_\parallel + \mathbf{g}$ and the energy of motion parallel to the surface $E_\parallel^{(\mathbf{g})}$ is equal to $\hbar^2(\mathbf{k}_\parallel + \mathbf{g})^2/2m$. Bearing in mind that the kinematics of elastic scattering must obey the energy-conservation law, we find that the energy of motion of the electron in the direction normal to the surface $E_z^{(\mathbf{g})}$ is given by $E_\parallel^{(0)} + E_z^{(0)} - E_\parallel^{(\mathbf{g})}$, which is equal to $\hbar^2 K_\mathbf{g}^2/2m$, where $K_\mathbf{g}^2 = \mathbf{k}^2 - (\mathbf{k}_\parallel + \mathbf{g})^2$. Taking account of the fact that there exists no condition determining the sign of the quantity $E_z^{(\mathbf{g})}$, we can distinguish between three possible cases: case (I) when $K_\mathbf{g}^2 > 0$, case (II) when $K_\mathbf{g}^2 = 0$, and case (III) when $K_\mathbf{g}^2 < 0$. The case that is realized in a particular experiment depends on the mutual orientation of the wave vector $\mathbf{k}$ of the incident electron beam and the reciprocal-lattice vector $\mathbf{g}$. In case (I), the side beam is reflected back into vacuum, in case (II), the side beam propagates in the direction parallel to the surface, and in case (III) (which corresponds to negative $E_z^{(\mathbf{g})}$, the side beam becomes evanescent, *i.e.* the component of the wave function associated with it attenuates exponentially in the vacuum region so that the corresponding diffraction spot disappears below the shadow edge. We use the term 'resonance scattering' to describe peaks in the intensity of the specular beam, which are often observed in the geometry of scattering corresponding to case (III), *i.e.* to $E_z^{(\mathbf{g})} < 0$.

Recently, Dudarev & Whelan (1993, 1995) have shown that the existence of a band of tightly bound one-dimensional states localized in the potential wells corresponding to atomic planes parallel to the surface gives rise to a resonance enhancement of the intensity of the specular beam at $E_z^{(\mathbf{g})} \simeq \varepsilon_0$, where $\varepsilon_0 < 0$ is the energy of the centre of the band. Generalizing these arguments, we can show that, in the case where there are n well separated bands of tightly bound states in the one-dimensional potential $U_0(z)$ situated at negative $\varepsilon = \varepsilon_0, \ldots, \varepsilon_n$, there exist n resonance peaks the positions of which correspond to $E_z^{(\mathbf{g})} \simeq \varepsilon_0, \ldots, \varepsilon_n$. Proceeding further, we may say that it is reasonable to expect that the positions of the resonance peaks are related to the positions of the peaks of the one-dimensional density of states associated with the potential $U_0(z)$ and corresponding to negative values of the energy $E_z^{(\mathbf{g})}$. The results obtained from the study of the tight-binding model also suggest that the relative heights

of the peaks depend on parameters determining the strength of resonance coupling between two rods involved in the process of scattering at a particular angle of incidence and on the magnitude of the imaginary part of the potential. Below, we present some arguments following from the results of both analytical and numerical studies of the equations of the theory of RHEED, which confirm the qualitative considerations given above.

3. Resonance scattering from the optical potential

We start from an analytical study of the integral equations of the theory of RHEED describing elastic scattering of high-energy electrons from a crystal surface. We make no assumption regarding the spectrum of the states involved in the process of resonance scattering, so that our conclusions remain valid both in the case of tight binding as well as in the weak-coupling limit. Our treatment is based on a theorem according to which, for an arbitrary one-dimensional Schrödinger equation, its Green function can be expressed in the form of a linear combination of two independent solutions of this equation. Using this theorem, we show that the Wronskian of those two linearly independent solutions is, on the one hand, a quantity the imaginary part of which is related to the effective one-dimensional density of states of the Hamiltonian and, on the other hand, a parameter that determines the magnitude of the resonance contribution to the surface reflectivity. Finally, we derive a simple analytical formula for the amplitude of resonance scattering, which makes it possible to separate the contributions to the surface reflectivity resulting from processes involving surface and bulk states in the one-dimensional potential $U_0(z)$ and to answer the question about the origin of the resonance parabolas present in RHEED patterns.

Representing the wave function $\Psi(\mathbf{r})$ of the high-energy electron as a two-dimensional series

$$\Psi(\mathbf{r}) = \sum_{\mathbf{g}'} \Phi_{\mathbf{g}'}(z) \exp[i(\mathbf{k}_\parallel + \mathbf{g}') \cdot \mathbf{R}] \tag{2}$$

and employing the two-rod approximation (Ohtsuki, 1968), we arrive at a system of two integral equations describing resonance diffraction of high-energy electrons from a crystal surface (Dudarev & Whelan, 1994*a*,*b*, 1995):

$$\Phi_0(z) = \Phi^{(+)}_{K_0}(z) + \int \mathrm{d}z' G(z, z', \hbar^2 K_0^2/2m) U_{-\mathbf{g}}(z') \Phi_{\mathbf{g}}(z')$$
$$\Phi_{\mathbf{g}}(z) = \int \mathrm{d}z' G(z, z', \hbar^2 K_{\mathbf{g}}^2/2m) U_{\mathbf{g}}(z') \Phi_0(z'), \tag{3}$$

where $K_{\mathbf{g}}^2 = \mathbf{k}^2 - (\mathbf{k}_\parallel + \mathbf{g})^2$ and $K_0^2 = k_z^2$. In (3), the wave function $\Phi^{(+)}_{K_0}(z)$ is the solution of the one-dimensional problem of diffraction

$$-(\hbar^2/2m)[\partial^2 \Phi^{(+)}_{K_0}(z)/\partial z^2] + U_0(z)\Phi^{(+)}_{K_0}(z) = (\hbar^2 K_0^2/2m)\Phi^{(+)}_{K_0}(z), \tag{4}$$

satisfying the asymptotic condition at $z \to -\infty$

$$\Phi^{(+)}_{K_0}(z) = \exp(iK_0 z) + R_0^{(\mathrm{pot})} \exp(-iK_0 z) \tag{5}$$

and $G(z, z', E)$ is the Green function of the Schrödinger equation of the form

$$\{E - [-(\hbar^2/2m)(\partial^2/\partial z^2) + U_0(z)]\} G(z, z', E) = \delta(z - z'). \tag{6}$$

In the limiting case where the Fourier components of the potential $U_{\pm\mathbf{g}}(z)$ giving rise to lateral momentum transfer can be considered as a perturbation (this may, for example, correspond to the case of relatively high temperatures), the amplitude of the specular reflection can be found using the one-dimensional distorted-wave approximation as

$$R_0 = R_0^{(\mathrm{pot})} + R_0^{(\mathrm{res})}, \tag{7}$$

where

$$R_0^{(\mathrm{res})} = -(im/\hbar^2 K_0) \int\int \mathrm{d}z\, \mathrm{d}z' \Phi^{(+)}_{K_0}(z) \times U_{-\mathbf{g}}(z) G(z, z', \hbar^2 K_{\mathbf{g}}^2/2m) U_{\mathbf{g}}(z') \Phi^{(+)}_{K_0}(z'). \tag{8}$$

Equation (7) shows that there exist two processes of scattering contributing to the amplitude of the specular beam. The first (the so-called 'potential', *i.e.* non-resonance) contribution results from diffraction of electrons by the one-dimensional potential $U_0(z)$. The magnitude of $R_0^{(\mathrm{pot})}$ depends only on the glancing angle of incidence and is independent of azimuth. The second ('resonance') contribution results from the process of virtual scattering *via* the states corresponding to negative energy $E_z^{(\mathbf{g})} = \hbar^2 K_{\mathbf{g}}^2/2m < 0$, which is associated with momentum transfers $\hbar\mathbf{g}$ and $-\hbar\mathbf{g}$ is the direction parallel to the surface. To avoid misunderstanding, we should emphasize that both $R_0^{(\mathrm{pot})}$ and $R_0^{(\mathrm{res})}$ result from scattering of electrons by the same potential $U(\mathbf{r})$, and in separating these two terms we follow a standard convention of the theory of scattering [see *e.g.* the treatises by Taylor (1972) and by Goldberger & Watson (1964) where this point is discussed in considerable detail] in which in the vicinity of a resonance peak the amplitude of scattering is separated into a rapidly varying 'resonance' part and a more slowly varying 'potential' part.

As follows from (8), the magnitude of the resonance contribution to the surface reflectivity depends on the form of the Green function $G(z, z', \hbar^2 K_{\mathbf{g}}^2/2m)$ describing one-dimensional propagation of the electron of energy $\hbar^2 K_{\mathbf{g}}^2/2m$ in the potential field $U_0(z)$, and evaluation of the double integral in (8) requires studying the properties of this Green function. We start by evaluating this function in the crystal bulk, *i.e.* in the limiting case

$z, z' \to \infty$, where $U_0(z)$ can be considered as a periodic function of z. The Green function $G(z, z', \hbar^2 K_g^2/2m)$ satisfies (6) in which $E = \hbar^2 K_g^2/2m$. Bearing in mind that any solution of (6) must satisfy the reciprocity condition [which follows from the fact that $\delta(z)$ is an even function of its argument],

$$G(z, z', \hbar^2 K_g^2/2m) = G(z', z, \hbar^2 K_g^2/2m), \qquad (9)$$

and also that for $z \neq z'$ it must be proportional to one of the two linearly independent Bloch waves $b_\kappa(z)$ or $b_{-\kappa}(z)$, which describe propagation of the electron in the potential $U_0(z)$, we arrive at (for $z, z' \to \infty$)

$$G_\infty(z, z', \hbar^2 K_g^2/2m) = \{2m/\hbar^2 W[b_{-\kappa}(z), b_\kappa(z)]\} \times \begin{cases} b_\kappa(z) b_{-\kappa}(z') & \text{when } z > z' \\ b_{-\kappa}(z) b_\kappa(z') & \text{when } z < z', \end{cases} \qquad (10)$$

where $W[b_{-\kappa}(z), b_\kappa(z)]$ is the Wronskian of the two Bloch functions $b_{-\kappa}(z)$ and $b_\kappa(z)$ of energy $\hbar^2 K_g^2/2m$, namely $W[b_{-\kappa}(z), b_\kappa(z)] = b_{-\kappa}(z) b'_\kappa(z) - b_\kappa(z) b'_{-\kappa}(z)$, which, since the Schrödinger equation does not contain the first-order derivative, is independent of z (Jeffreys & Jeffreys, 1950). The presence of the surface results in reflection of Bloch states back into the crystal bulk and the Green function acquires the form (for $z > z_0$)

$$G(z, z', \hbar^2 K_g^2/2m) = G_\infty(z, z', \hbar^2 K_g^2/2m) + \mathcal{R}(K_g)\{2m/\hbar^2 W[b_{-\kappa}(z), b_\kappa(z)]\} \times b_\kappa(z) b_\kappa(z'), \qquad (11)$$

where $\mathcal{R}(K_g)$ is the amplitude of the coefficient of reflection for the Bloch waves incident on the crystal surface from inside (*i.e.* from $z \to +\infty$). The magnitude of $\mathcal{R}(K_g)$ is determined by the condition of continuity of the Green function and its derivative at any point in the interfacial region between vacuum and the crystal:

$$\mathcal{R}(K_g) = -\left[\frac{\varphi_{K_g}(z_0) b'_{-\kappa}(z_0) - \varphi'_{K_g}(z_0) b_{-\kappa}(z_0)}{\varphi_{K_g}(z_0) b'_\kappa(z_0) - \varphi'_{K_g}(z_0) b_\kappa(z_0)}\right], \qquad (12)$$

where z_0 is the coordinate of a point to the right of which the potential $U_0(z)$ can be considered as being periodic, and $\varphi_{K_g}(z)$ is a solution of the Schrödinger equation (4) satisfying the asymptotic condition $\varphi_{K_g}(z) \simeq \exp(-iK_g z)$ in the limit $z \to -\infty$. The poles of $\mathcal{R}(K_g)$ lying on the positive imaginary axis in the complex plane of K_g correspond to surface states localized at the interface between vacuum and the crystal (Davison & Steślicka, 1992) and can therefore be used as a means of identification of those states. Substituting (11) into (8), we arrive at

$$R_0^{(\mathrm{res})} = -i\{2m^2/\hbar^4 K_0 W[b_{-\kappa}(z), b_\kappa(z)]\} \times \left[\int_{-\infty}^{\infty} \int_{-\infty}^{z} dz\, dz' \Phi_{K_0}^{(+)}(z) U_{-g}(z) b_\kappa(z) b_{-\kappa}(z') \times U_g(z') \Phi_{K_0}^{(+)}(z') + \int_{\infty}^{\infty} \int_{z}^{\infty} dz\, dz' \Phi_{K_0}^{(+)}(z) U_{-g}(z) b_{-\kappa}(z) b_\kappa(z') \times U_g(z') \Phi_{K_0}^{(+)}(z') + \mathcal{R}(K_g) \int_{-\infty}^{\infty} \int_{-\infty}^{\infty} dz\, dz' \Phi_{K_0}^{(+)}(z) U_{-g}(z) b_\kappa(z) b_\kappa(z') \times U_g(z') \Phi_{K_0}^{(+)}(z') \right]. \qquad (13)$$

Examination of this equation shows that it is possible to identify all the basic parameters that influence the magnitude of the resonance part of the surface reflectivity. Firstly, the amplitude of $R_0^{(\mathrm{res})}$ is proportional to

$$1/W[b_{-\kappa}(z), b_\kappa(z)],$$

where $W[b_{-\kappa}(z), b_\kappa(z)]$ is the Wronskian of two linearly independent Bloch functions corresponding to the energy $\hbar^2 K_g^2/2m$. As is shown in the Appendix, the imaginary part of $W^{-1}[b_{-\kappa}(z), b_\kappa(z)]$ is proportional to the one-dimensional effective density of bulk states associated with the optical potential $U_0(z)$. Secondly, the amplitude of the resonance contribution to the

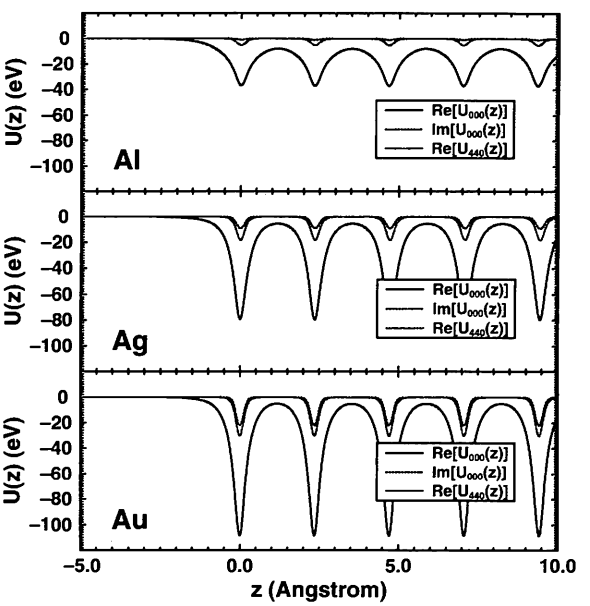

Fig. 2. Profiles of the laterally averaged potential of Al(111), Ag(111) and Au(111) atomic planes for $T = 293$ K. Solid curve: the real part of the potential $U'_0(z)$ evaluated as a sum of five Doyle–Turner terms taken from Dudarev *et al.* (1995). Dotted curve: the imaginary part of the potential $U''_0(z)$ evaluated as a sum of five Doyle–Turner terms taken from the same source.

surface reflectivity depends on the magnitude of matrix elements of the form

$$\int dz \Phi^{(+)}_{K_0}(z) U_{\pm \mathbf{g}}(z) b_{\pm\kappa}(z), \qquad (14)$$

describing the coupling between two resonating Bloch states $\Phi^{(+)}_{K_0}(z)$ and $b_{\pm\kappa}(z)$, which correspond to the two rods involved in the process of scattering. This matrix element depends on the extent of the overlap of the Bloch states $\Phi^{(+)}_{K_0}(z)$ and $b_{\pm\kappa}(z)$ with the Fourier components of the potential $U_{\pm\mathbf{g}}(z)$ (the latter quantities are in most cases localized in the vicinity of the centres of atomic planes parallel to the surface of the crystal, see Fig. 2). The third factor affecting the amplitude of the resonance contribution to the reflectivity is the presence or absence of surface states, *i.e.* the existence of poles of the function $\mathcal{R}(K_g)$ in the upper half-plane of the complex variable K_g.

In the following section, we discuss the results of numerical calculations of the resonance reflectivity of various crystal surfaces and show that in all cases examined the positions of the peaks of the effective one-dimensional density of states {*i.e.* the peaks of the imaginary part of $W^{-1}[b_{-\kappa}(z), b_{\kappa}(z)]$, considered as a function of $\hbar^2 K_g^2/2m$ for negative values of this quantity} correspond to the positions of the resonance peaks of the specular-beam intensity.

4. Numerical results and discussion

All the computational results described in this section have been obtained using the R-matrix method, the previous applications of which have been described earlier by Dudarev & Whelan (1994*b*) and Dudarev, Peng & Whelan (1995) and which has recently been verified against the numerical techniques developed by other groups (Ichimiya, 1995). To ensure the reliability of the parameters that we used in our calculations, we compare rocking curves calculated using our program for the Pt (111) surface with experimental data obtained by Marten & Meyer-Ehmsen (1985) (see Fig. 3). All the parameters entering numerical calculations have been evaluated from first principles following the procedure developed by Dudarev *et al.* (1995) to estimate the effect of phonon scattering and by Ritchie & Howie (1977) to take into account electronic excitations. No fitting procedure has been employed. Despite visible disagreement between absolute intensities (it should be noted that it is likely that experimental intensities have been affected by the presence of surface roughness), the positions of peaks in all curves agree very well. In what follows, we use numerical results obtained using the same computer program to verify the conclusions that follow from the analytical consideration of resonance scattering given above.

As an example, we consider scattering from the (111) surfaces of three f.c.c. crystals, namely aluminium ($Z = 13$), silver ($Z = 47$) and gold ($Z = 79$). The lattice constants of these crystals ($a_{Al} = 4.05$, $a_{Ag} = 4.09$, $a_{Au} = 4.08$ Å) do not differ by more than 1%. This makes them particularly suitable for the analysis of the effects of the variation of the strength of the interaction potential and the associated changes in the band structure on the positions and intensities of the resonance peaks.

We start by considering Bragg scattering of electrons from the one-dimensional potential $U_0(z)$ shown in Fig. 2. In the absence of momentum transfer parallel to the surface, the intensity of the specular reflection is independent of azimuth and represents the 'potential' part of the reflection coefficient $R_0^{(pot)}$ of (7). The dependence of the amplitude of the specular beam $|R_0^{(pot)}|$ on the glancing angle of incidence ζ is shown in Fig. 4 for all three crystals, together with the density of states $D(E) = D(\hbar^2 K_0^2/2m)$ calculated using (20) at zero temperature. The Bloch states have been found by diagonalizing transfer matrices describing propagation of the electron wave function through an individual bulk layer of atoms. As follows from the results shown in Fig. 4, in the case of one-dimensional diffraction the positions of the peaks in the rocking curves (*i.e.* in the curves showing the dependence of the reflectivity on the angle of incidence) coincide with the position of forbidden gaps in the spectrum of one-dimensional density of states. This fact is well known in diffraction

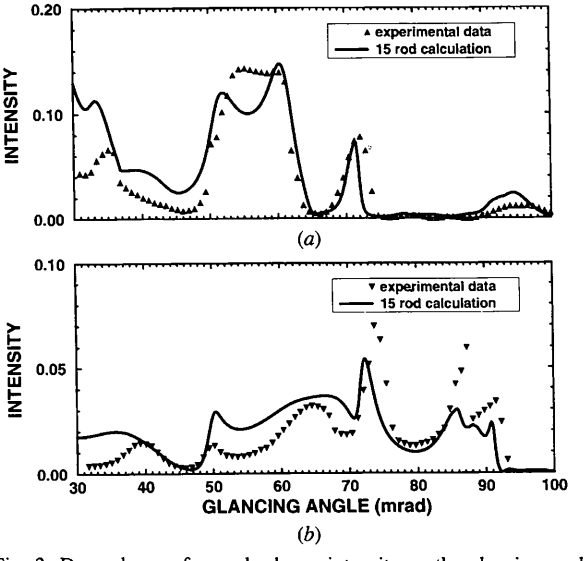

Fig. 3. Dependence of specular-beam intensity on the glancing angle of incidence ζ calculated numerically for the Pt (111) surface and $E = 19$ keV. (*a*) The incident-beam azimuth is along ⟨110⟩ and the corresponding experimental rocking curve is taken from Fig. 1(*a*) of Marten & Meyer-Ehmsen (1985). (*b*) The incident-beam azimuth is 29.3 mrad away from ⟨11$\bar{2}$⟩ and the corresponding experimental rocking curve is taken from Fig. 1(*c*) of Marten & Meyer-Ehmsen (1985). 15 rods of the zero-order Laue zone have been employed (the zero-order rod and seven rods on either side of it) in the evaluation of the specular-beam intensity.

theory and is often used as an illustration of the statement that the incident beam of electrons is reflected back into vacuum if the Bloch wave corresponding to the energy $E_z^{(0)} = \hbar^2 K_0^2/2m$ becomes evanescent and cannot propagate into the crystal bulk.

To understand the behaviour of the resonance part of the reflectivity $R^{(\mathrm{res})}$ from (8), we analyse the dependence of the intensity of the specular beam as a function of the azimuthal angle η. Introducing spherical coordinates and representing the wave vector of the incident electrons $\mathbf{k}$ in the form $\mathbf{k} = (k\cos\zeta\cos\eta, k\cos\zeta\sin\eta, k\sin\zeta)$, we obtain $E_z^{(0)} = (\hbar^2k^2/2m)\sin^2\zeta$ and

$$E_z^{(\mathbf{g})} = \hbar^2 K_{\mathbf{g}}^2/2m = (\hbar^2k^2/2m)[\sin^2\zeta - 2(g/k)\cos\zeta\sin\eta - (g^2/k^2)], \tag{15}$$

where we have assumed that vector $\mathbf{g}$ is parallel to the y axis. Equation (15) shows that, by varying the azimuthal angle η, we can tune the value of $E_z^{(\mathbf{g})}$ while at the same time not affecting the magnitude of $E_z^{(0)}$. In other words, by analysing the dependence of the intensity of the specular beam as a function of the azimuthal angle η and keeping the glancing angle of incidence ζ constant, we can identify the peaks of the reflectivity associated with pure resonance scattering [the second term in (7)]. To avoid strong effects resulting from interference between resonance and potential scattering [for the discussion of these effects see Dudarev & Whelan (1995)], we consider the values of the glancing angle of incidence ζ, corresponding to one of the minima of the intensity of the one-dimensional rocking curves shown in Fig. 4. For $\hbar^2k^2/2m = 100\,\mathrm{keV}$, the positions of the minima of the intensity in the rocking curves are $\zeta = 58.8\,\mathrm{mrad}$ for Al [midway between the (777) and (888) horizontal Kikuchi lines], $\zeta = 65.3\,\mathrm{mrad}$ for Ag [midway between the (888) and (999) horizontal Kikuchi lines] and $\zeta = 65.0\,\mathrm{mrad}$ for Au [midway between the (888) and (999) horizontal Kikuchi lines]. A set of curves illustrating the behaviour of the resonance part of the reflectivity as a function of $\hbar^2K_{\mathbf{g}}^2/2m$, which have been computed by varying the azimuthal angle η [which is related to $\hbar^2K_{\mathbf{g}}^2/2m$ *via* (15)], is shown in Figs. 5–7 for the (111) surfaces of Al, Ag and Au, together with the curves showing the dependence of the density of states $D(E)$ and the effective density of states $D_{\mathrm{eff}}(E)$ (see Appendix) on energy for negative values of $\hbar^2K_{\mathbf{g}}^2/2m$.

The most striking difference between the curves shown in Figs. 5–7 and those of Fig. 4 is that the peaks of the resonance part of the reflectivity generally coincide with the peaks of the one-dimensional density of states rather than with forbidden gaps

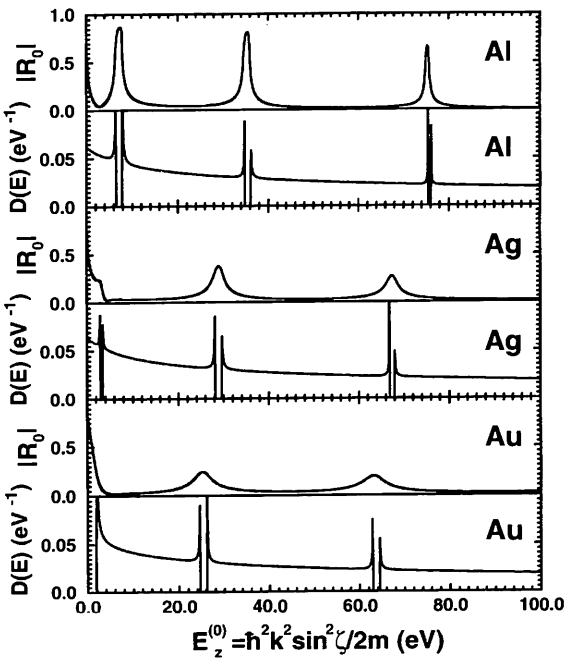

Fig. 4. The potential contribution to the surface reflectivity for the Al(111), Ag(111) and Au(111) surfaces (according to its definition, this contribution results from one-dimensional scattering of electrons by the laterally averaged potential of the crystal) and the corresponding one-dimensional densities of states plotted as a function of the energy of motion in the direction normal to the surface. Energy of electrons $E = 100\,\mathrm{keV}$ and the absolute temperature $T = 293\,\mathrm{K}$.

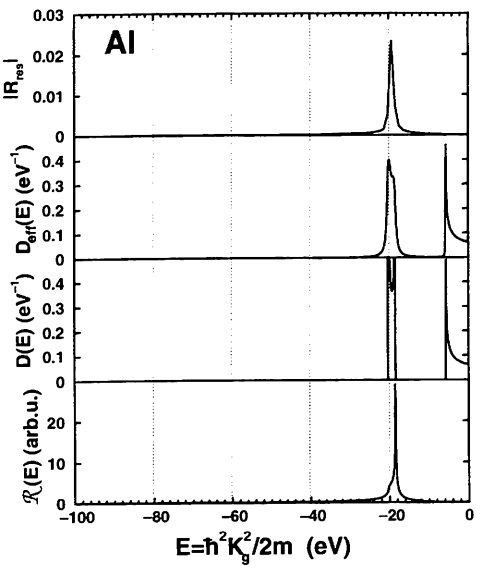

Fig. 5. The resonance contribution to the surface reflectivity, the density of states $D(E)$, the effective density of states $D_{\mathrm{eff}}(E)$ and the amplitude of the coefficient of internal reflection $\mathcal{R}$ of Bloch waves from the surface calculated for the Al(111) surface as a function of energy $E_z^{(\mathbf{g})}$, which is related to the azimuthal angle η by (15). $\eta = 0$ corresponds to the $\langle 11\bar{2}\rangle$ azimuth. The interval of energies $\hbar^2K_{\mathbf{g}}^2/2m$ from -100 to $0.0\,\mathrm{eV}$ corresponds to an interval of azimuthal angles η from 18.2 to 7.4 mrad.

as in the case of one-dimensional diffraction. This result is entirely consistent with the solution of the tight-binding model (Dudarev & Whelan, 1994*a*,*b*), where the density of states has the form of a δ-function peak situated at ε_0, and the coefficient of resonance reflection reaches its maximum in the vicinity of $\hbar^2 K_g^2/2m = \varepsilon_0$. In more qualitative terms, the link between the effective density of states and the resonance reflectivity results from the fact that the resonance channel of scattering is associated with scattering *via* some intermediate states, and this requires the very existence of these intermediate states for the resonance part of the reflectivity to be substantial.

It should be emphasized that the purely tight-binding description is not capable of describing all the resonance peaks shown in Figs. 5–7, which represent horizontal tracks across the pattern similar to that shown in Fig. 1. In each figure, it is only the left-hand peak that is associated with the states tightly bound by the potential of adjacent planes of atoms. The second peaks on the right-hand side of the diagrams shown in Figs. 6 and 7 correspond to energies that exceed the maximum of the potential $U_0(z)$ shown in Fig. 2 and therefore the relevant Bloch states involved in the formation of a virtual resonance state are highly delocalized in real space.

The only deviation from the rule establishing a correspondence between the position of resonance features and the effective density of bulk states, which can be noticed by examining the curves shown in Figs. 5–7, is that the second peak of the density of states for aluminium situated at $E_z^{(g)} \simeq -6\,\text{eV}$ does not correspond to any peak in the curve showing the azimuthal dependence of the resonance part of the reflectivity. However, this deviation can be easily explained by comparing the energy dependence of $D(E)$ and $D_{\text{eff}}(E)$ in the vicinity of $E \simeq -6\,\text{eV}$, where it is seen that the density of states $D(E)$ is almost insensitive to the presence of the imaginary part of the potential. This fact shows that the Bloch states, which contribute to the density of states in this region of energy, have nodes in the vicinity of the centres of atomic planes. This leads to the vanishing of the matrix element (14), which determines the strength of coupling between two resonating Bloch states and the very possibility of appearance of the corresponding resonance peak in a rocking curve.

The remaining question concerns the contribution to the reflectivity resulting from resonance scattering *via* surface states, *i.e.* the contribution of the type discussed in detail by McRae (1979). To identify the energies of the surface states, in Figs. 5–7 we have plotted the dependence of the coefficient $\mathcal{R}$ of internal reflection of one-dimensional Bloch waves from the surface (12) for negative values of $\hbar^2 K_g^2/2m$, and for the case where the imaginary

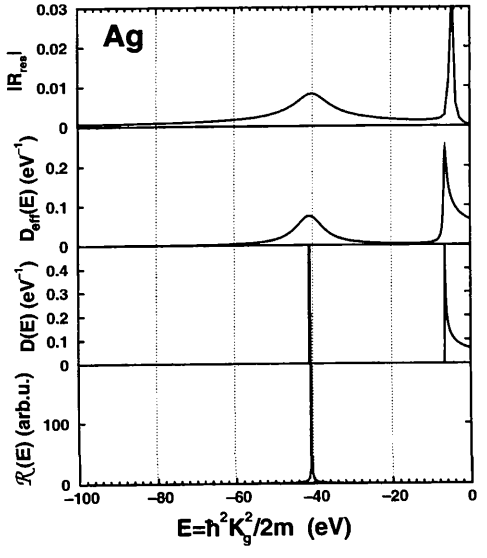

Fig 6. The resonance contribution to the surface reflectivity, the density of states $D(E)$, the effective density of states $D_{\text{eff}}(E)$ and the amplitude of the coefficient of internal reflection $\mathcal{R}$ of Bloch waves from the surface calculated for the Ag(111) surface as a function of energy $E_z^{(g)}$, which is related to the azimuthal angle η by (15). $\eta = 0$ corresponds to the $\langle 11\bar{2}\rangle$ azimuth. The interval of energies $\hbar^2 K_g/2m$ from -100 to 0.0 eV corresponds to an interval of azimuthal angles η from 26.7 to 15.9 mrad.

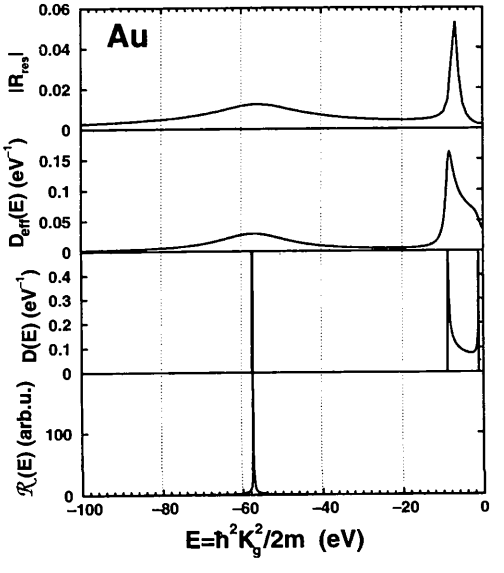

Fig. 7. The resonance contribution to the surface reflectivity, the density of states $D(E)$, the effective density of states $D_{\text{eff}}(E)$ and the amplitude of the coefficient of internal reflection $\mathcal{R}$ of Bloch waves from the surface calculated for the Au(111) surface as a function of energy $E_z^{(g)}$, which is related to the azimuthal angle η by (15). $\eta = 0$ corresponds to the $\langle 11\bar{2}\rangle$ azimuth. The interval of energies $\hbar^2 K_g/2m$ from -100 to 0.0 eV corresponds to an interval of azimuthal angles η from 26.2 to 15.3 mrad.

part of the potential $U_0(z)$ vanishes. As follows from some general theorems of the theory of scattering, the poles of $\mathcal{R}(K_g)$ situated in the upper half-plane of the complex variable K_g give the energies of the surface states localized at the interface between the crystal and vacuum. This view contrasts with a previous proposal made by Peng (1994), where the existence of a surface state was linked to a singularity of an (external) reflection coefficient for a real value of the wave vector. As follows from the results shown in Figs. 5–7, in all the three cases considered here [namely Al(111), Ag(111) and Au(111) surfaces], the surface states do exist and their energies almost coincide with the upper edge of the lowest band of the bulk states. The origin of those surface states is associated with the slight deviation of the form of the potential of the outer layer of atoms from that of a bulk layer. Can we say that these states are responsible for the appearance of the resonance peaks of the reflectivity? There are two reasons why the answer to this question should be negative. The first is that, as follows from examination of the curves shown in Figs. 5–7, the number of resonance peaks of the reflectivity exceeds the number of surface states, and some of the resonance peaks do not correspond to any surface at all. The second is that even in the case where the energy of the surface state and the position of the resonance peak almost coincide, the effective inelastic width of both the surface and bulk states [see *e.g.* the curves showing the dependence of $D_{\text{eff}}(E)$ on energy E] exceeds many times the characteristic energy separation between the surface state and the upper edge of the band of bulk states making them indistinguishable, and therefore making meaningless the question of separation of the contributions of all these states to the intensity of the specular beam.

Our final comment concerns the interpretation of the results of numerical calculations performed by Peng (1994). As follows from examination of the curves shown in Figs. 2(*c*) and 3(*c*) of the paper by Peng (1994), the intensity of the specular beam is a maximum in the region between two singularities in the Bloch-wave excitation amplitudes. Taking into account that in the case considered by Peng (1994) all the features in the rocking curves are slightly shifted owing to the finiteness of the matrix element of resonance coupling between two rods, we can conclude that the singularities shown in Figs. 2(*c*) and 3(*c*) of Peng (1994) are in fact associated with singularities of the density of states at the band edges similar to those shown in Fig. 4 of the present paper. The origin of the resonance peaks shown in Figs. 2(*d*) and 3(*d*) of Peng (1994) can therefore be attributed to resonance scattering *via* Bloch states belonging to a band situated at negative $E_z^{(g)}$, a conclusion entirely in agreement with the considerations of the present paper.

5. Conclusions

In this paper, we have presented some qualitative, analytical and numerical arguments that make it possible to classify the processes leading to resonance scattering of high-energy electrons from surfaces. We have proposed that the factor that is primarily responsible for the appearance of the resonance maxima of the surface reflectivity is the existence of peaks in the effective density of bulk states corresponding to one-dimensional motion of the electrons in the direction normal to the surface. This is in contrast to the case of Bragg diffraction, where the peaks of the reflectivity correspond to forbidden gaps in the spectrum of Bloch states. We have also shown that the intensities of the resonance peaks depend on the values of the matrix elements describing resonance coupling between two Bloch states, and that in all the cases considered the effects associated with the existence of surface states are unimportant.

The preparation of this paper has been stimulated by discussions and correspondence with A. Howie and K. Kambe, to whom we express our sincere thanks. We are also grateful to L.-M. Peng for fruitful discussions and helpful comments. SLD acknowledges financial support of this work from the University of Oxford. Numerical computations have been performed using the facilities of the Materials Modelling Laboratory, Department of Materials, University of Oxford, which was funded in part by EPSRC grant no. GR/H 58278.

APPENDIX *A*

In this Appendix, we derive a simple formula relating one-dimensional bulk density of states $D(E)$ and the Wronskian of two linearly independent solutions of the Schrödinger equation corresponding to the energy E. Assuming the potential $U_0(z)$ to be real, we represent the Green function $G_\infty(z, z', E)$ in two equivalent forms:

$$\begin{aligned} G_\infty(z, z', E) &= \int_{-\infty}^{\infty} (\mathrm{d}q/2\pi)[b_q(z)b_{-q}(z')]/(E - \varepsilon_q + i0) \\ &= \{2m/\hbar^2 W[b_{-\kappa}(z), b_\kappa(z)]\} \\ &\quad \times \begin{cases} b_\kappa(z)b_{-\kappa}(z') & \text{when } z > z' \\ b_{-\kappa}(z)b_\kappa(z') & \text{when } z < z', \end{cases} \end{aligned} \tag{16}$$

where $\varepsilon_\kappa = E$ and we have taken into account that $b_q^*(z) = b_{-q}(z)$. The Bloch functions are normalized by the condition

$$\int_{z}^{z+d} \mathrm{d}\xi b_q(\xi) b_{-q}(\xi) = 1, \tag{17}$$

which is assumed to be satisfied for arbitrary z, and d is the lattice constant. Considering the imaginary part of the Green function,

$$\begin{aligned} \operatorname{Im} G_\infty(z, z, E) &= -\pi \int_{-\infty}^{\infty} (\mathrm{d}q/2\pi)\delta(E - \varepsilon_q) b_q(z) b_{-q}(z) \\ &= (2m/\hbar^2) \operatorname{Im}\{1/W[b_{-\kappa}(z), b_\kappa(z)]\} \\ &\quad \times b_\kappa(z) b_{-\kappa}(z), \end{aligned} \tag{18}$$

and taking into account the definition

$$D(E) = \int_{-\infty}^{\infty} (\mathrm{d}q/2\pi)\delta(E - \varepsilon_q), \tag{19}$$

we arrive at

$$D(E) = -(2m/\pi\hbar^2) \operatorname{Im}\{1/W[b_{-\kappa}(z), b_\kappa(z)]\}. \tag{20}$$

The latter definition can be extended to a more general case where the one-dimensional potential contains a non-vanishing imaginary part (*i.e.* to the case of the optical potential, which is often used to describe scattering of high-energy electrons by crystals [see *e.g.* Dudarev *et al.* (1992)]. Although (18) and (19) cannot be directly applied to this more general case, and therefore the relevant quantity should now be called the 'effective' density of states $D_{\mathrm{eff}}(E)$, numerical studies showed that the right-hand side of (20) remains a positive quantity. Fig. 8 illustrates the difference between the density of states $D(E)$ (which is the quantity corresponding to zero imaginary part of the potential) and the effective density of states $D_{\mathrm{eff}}(E)$ calculated for the potential of the Au(111) atomic planes using (20) and taking into account the imaginary part of the potential resulting from scattering of high-energy electrons by phonons at $T = 293$ K.

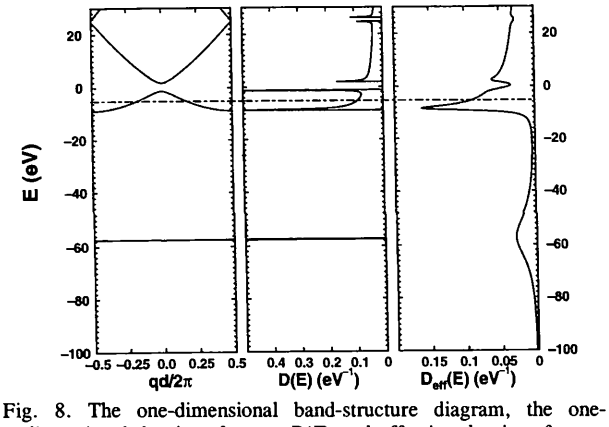

Fig. 8. The one-dimensional band-structure diagram, the one-dimensional density of states $D(E)$ and effective density of states $D_{\mathrm{eff}}(E)$ calculated for the potential of the Au(111) atomic planes. Note the marked difference between $D(E)$ and $D_{\mathrm{eff}}(E)$ resulting from absorption effects.

References

Bleloch, A. L., Howie, A., Milne, R. H. & Walls, M. G. (1989). *Ultramicroscopy*, **29**, 175–182.

Cowley, J. M. (1982). *Phys. Rev. B*, **25**, 1401–1404.

Davison, S. G. & Stęślicka, M. (1992). *Basic Theory of Surface States*. Oxford: Clarendon Press.

Dudarev, S. L., Peng, L.-M. & Whelan, M. J. (1992). *Surf. Sci.* **279**, 380–394.

Dudarev, S. L., Peng, L.-M. & Whelan, M. J. (1995). *Surf. Sci.* **330**, 86–100.

Dudarev, S. L. & Whelan, M. J. (1993). *Electron Microscopy and Analysis 1993. Inst. Phys. Conf. Ser.* Vol. 138, edited by A. J. Craven, pp. 217–220. Bristol/Philadelphia: Institute of Physics Publishing.

Dudarev, S. L. & Whelan, M. J. (1994*a*). *Phys. Rev. Lett.* **72**, 1032–1035.

Dudarev, S. L. & Whelan, M. J. (1994*b*). *Surf. Sci.* **310**, 373–389.

Dudarev, S. L. & Whelan, M. J. (1994*c*). *Electron Microscopy 1994. Proceedings of the 13th International Congress on Electron Microscopy*, Vol. 1, edited by B. Jouffrey & C. Colliex, pp. 949–950. Paris: Les Editions de Physique.

Dudarev, S. L. & Whelan, M. J. (1995). *Surf. Sci.* **340**, 293–308.

Dudarev, S. L. & Whelan, M. J. (1996). *Int. J. Mod. Phys.* **10**, 133–168.

Echenique, P. M. & Pendry, J. B. (1989). *Prog. Surf. Sci.* **32**, 111–172.

Gajdardziska-Josifovska, M. & Cowley, J. M. (1991). *Acta Cryst.* A**47**, 74–82.

Goldberger, M. L. & Watson, K. M. (1964). *Collision Theory*, Ch. 8. New York: Wiley.

Horio, Y. & Ichimiya, A. (1996). *Surf. Sci.* **348**, 344–358.

Ichimiya, A. (1995). Private communication.

Ichimiya, A., Kambe, K. & Lehmpfuhl, G. (1980). *J. Phys. Soc. Jpn*, **49**, 684–688.

James, R. (1990). DPhil thesis, University of Bath, England.

James, R., Bird, D. M. & Wright, A. G. (1989). *EMAG-MICRO89. Inst. Phys. Conf. Ser.* Vol. 98, edited by P. J. Goodhew & N. Y. Elder, pp. 111–114. Bristol/New York: Institute of Physics Publishing.

Jeffreys, H. & Jeffreys, B. S. (1950). *Methods of Mathematical Physics*, 2nd ed., p. 493. Cambridge University Press.

Kambe, K. (1967). *Z. Naturforsch. Teil A*, **22**, 422–431.

Kikuchi, S. & Nakagawa, S. (1933). *Sci. Pap. Inst. Phys. Chem. Res.* **21**, 256–265.

Larsen, P. K. & Dobson, P. J. (1987). Editors. *Reflection High Energy Electron Diffraction and Reflection Electron Imaging of Surfaces. NATO Advanced Study Institute, Series B: Physics*, Vol. 188. New York: Plenum Press.

Lehmpfuhl, G. & Dowell, W. C. T. (1986). *Acta Cryst.* A**42**, 569–577.

Ma, Y. & Marks, L. D. (1989). *Acta Cryst.* A**45**, 174–182.

McRae, E. G. (1979). *Rev. Mod. Phys.* **51**, 541–568.

Marten, H. & Meyer-Ehmsen, G. (1985). *Surf. Sci.* **151**, 570–584.

Meyer-Ehmsen, G. (1987). *Reflection High Energy Electron Diffraction and Reflection Electron Imaging of Surfaces. NATO Advanced Study Institute, Series B: Physics*, Vol. 188, edited by P. K. Larsen & P. J. Dobson, pp. 99–107. New York: Plenum Press.

Ohtsuki, Y. H. (1968). *J. Phys. Soc. Jpn*, **25**, 481–493.

Peng, L.-M. (1994). *Surf. Sci.* **316**, L1049–L1054.

Peng, L.-M. & Cowley, J. M. (1986). *Acta Cryst.* A**42**, 545–552.

Reginski, K., Lamin, M. A., Mashanov, V. I., Pchelyakov, O. P. & Sokolov, L. V. (1995). *Surf. Sci.* **327**, 93–99.

Ritchie, R. H. & Howie, A. (1977). *Philos. Mag.* **36**, 463–481.

Smith, A. E., Lehmpfuhl, G. & Uchida, Y. (1992). *Ultramicroscopy*, **41**, 367–373.

Spence, J. C. H. & Kim, Y. (1987). *Reflection High Energy Electron Diffraction and Reflection Electron Imaging of Surfaces. NATO Advanced Study Institute, Series B: Physics*, Vol. 188, edited by P. K. Larsen & P. J. Dobson, pp. 117–129. New York: Plenum Press.

Taylor, J. R. (1972). *Scattering Theory*, Ch. 13. New York: Wiley.

Wang, Z. L. (1989). *Philos. Mag.* B**60**, 617–626.

Zhao, T. C. & Tong, S. Y. (1993). *Phys. Rev. B*, **47**, 3923–3928.

Zuo, J. M. & Liu, J. (1992). *Surf. Sci.* **271**, 253–259.